Inorganic Chemistry

Forum Article

pubs.acs.org/IC

Chemical Speciation of Neptunium(VI) under Strongly Alkaline Conditions. Structure, Composition, and Oxo Ligand Exchange

David L. Clark,* Steven D. Conradson, Robert J. Donohoe,† Pamela L. Gordon, D. Webster Keogh, Phillip D. Palmer, Brian L. Scott, and C. Drew Tait

Los Alamos National Laboratory, Los Alamos, New Mexico 87545, United States

Supporting Information

ABSTRACT: Hexavalent neptunium can be solubilized in 0.5−3.5 M aqueous MOH (M = Li^+, Na^+, NMe_4^+ = TMA^+) solutions. Single crystals were obtained from cooling of a dilute solution of $Co(NH_3)_6Cl_3$ and NpO_2^{2+} in 3.5 M $[N(Me)_4]OH$ to 5 °C. A single-crystal X-ray diffraction study revealed the molecular formula of $[Co(NH_3)_6]_2[NpO_2(OH)_4]_3{\cdot}H_2O$, isostructural with the uranium analogue. The asymmetric unit contains three distinct $NpO_2(OH)_4^{2-}$ ions, each with pseudooctahedral coordination geometry with *trans*-oxo ligands. The average Np═O and Np−OH distances were determined to be 1.80(1) and 2.24(1) Å, respectively. EXAFS data and fits at the Np L_{III}-edge on solid $[Co(NH_3)_6]_2[NpO_2(OH)_4]_3{\cdot}H_2O$ and aqueous solutions of NpO_2^{2+} in 2.5 and 3.5 M (TMA)OH revealed bond lengths nearly identical with those determined by X-ray diffraction but with an increase in the number of equatorial ligands with increasing (TMA)OH concentration. Raman spectra of single crystals of $[Co(NH_3)_6]_2[NpO_2(OH)_4]_3{\cdot}H_2O$ reveal a ν_1(O═Np═O) symmetric stretch at 741 cm^{-1}. Raman spectra of NpO_2^{2+} recorded in a 0.6−2.2 M LiOH solution reveal a single ν_1 frequency of 769 cm^{-1}. Facile exchange of the neptunyl oxo ligands with the water solvent was also observed with Raman spectroscopy performed with ^{16}O- and ^{18}O-enriched water solvent. The combination of EXAFS and Raman data suggests that $NpO_2(OH)_4^{2-}$ is the dominant solution species under the conditions of study and that a small amount of a second species, $NpO_2(OH)_5^{3-}$, may also be present at higher alkalinity. Crystal data for $[Co(NH_3)_6]_2[NpO_2(OH)_4]_3{\cdot}H_2O$: monoclinic, space group *C*2/*c*, *a* = 17.344(4) Å, *b* = 12.177(3) Å, *c* = 15.273 Å, β = 120.17(2)°, *Z* = 4, R1 = 0.0359, wR2 = 0.0729.

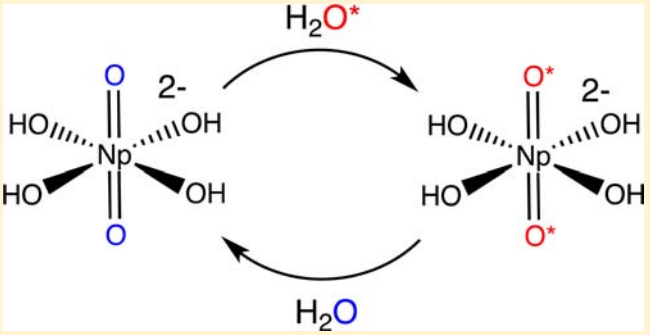

INTRODUCTION

From a historical perspective, the chemistry of actinide elements under highly alkaline solution conditions is relatively underdeveloped compared to the large body of literature on actinide behavior in strongly acidic to near-neutral conditions.[1−4] Recent scientific interest in the alkaline solution chemistry of transuranium (TRU) elements has been stimulated by the recognition that alkaline radioactive wastes exist in many countries, and knowledge of the nature of chemical species formed under these conditions is a prerequisite to remediation of these legacy wastes.[5−7] On the basis of all of the data amassed, it is clear that, under the strongly alkaline conditions characteristic of waste tanks and sludge washing conditions ($[OH^-]$ = 2−14 M), TRU elements can have significant solubility, causing difficulty in separations and partitioning into both high- and low-level waste components.

The stoichiometry, chemical composition, electronic structure, and highly unusual oxo ligand exchange of the uranyl(VI) ion in strongly alkaline solutions have been the subject of significant study over the past decade. In 1999, we reported on the crystal structure of $UO_2(OH)_4^{2-}$ and a variety of spectroscopic data that indicated an equilibrium between $UO_2(OH)_4^{2-}$ and $UO_2(OH)_5^{3-}$ in solution, accompanied by chemical exchange between the oxygen atoms of the uranyl(VI) unit and the oxygen atoms in the water solvent.[8] While the composition of $UO_2(OH)_4^{2-}$ in the solid state and its associated axial U═O and equatorial U−OH bond distances and vibrational frequencies were undisputed, subsequent extended X-ray absorption fine structure (EXAFS) data from several groups gave rise to differing interpretations as to the identity of the limiting species in solution, with our data suggesting $UO_2(OH)_5^{3-}$ based on EXAFS and a hydroxide dependence of UV−vis and luminescence spectra,[8] while Grenthe and co-workers argued for $UO_2(OH)_4^{2-}$ based on comparisons of EXAFS with quantum-chemical calculations.[9−11] A portion of the debate centered on the expectation that equatorial U−OH bond lengths should increase with increasing equatorial coordination number from 4 to 5, yet the EXAFS data gave essentially identical U═O and U−OH distances for both species. During the course of the debate, our

Special Issue: Inorganic Chemistry Related to Nuclear Energy

Received: September 16, 2012
Published: March 13, 2013

   dx.doi.org/10.1021/ic3020139 | Inorg. Chem. 2013, 52, 3547−3555

original evidence for oxo ligand exchange was first questioned[10] and later confirmed by Grenthe and Szabo.[12] In the most recent report, Grenthe and Szabo reported a series of elegant ^{17}O NMR studies that confirmed our proposal that both $UO_2(OH)_4^{2-}$ and $UO_2(OH)_5^{3-}$ were present in solution and that oxo ligand exchange takes place via axial "yl" oxygen atoms and equatorial hydroxides.[12] The conundrum over the identical equatorial U−OH bond lengths was never satisfactorily explained. The experimental findings generated much quantum-chemical interest in the structure of the ions, the nature of the oxo atom exchange mechanism, and the energetics of possible intermediates.[13−17] The calculations identified that π bonding of equatorial OH^- ligands in $UO_2(OH)_4^{2-}$ results in a weaker axial U=O bond and that equatorial π bonding with OH^- ligands is less important for $UO_2(OH)_5^{3-}$.[13−17]

The decade-long discussion surrounding the behavior of the uranyl(VI) ion in alkaline solutions raises obvious questions about the composition, structure, and possible ligand exchange in the corresponding neptunyl(VI) system. There have been several studies on the solution composition of the unstable heptavalent $AnO_4(OH)_2^{3-}$ ion that decomposes to hexavalent $AnO_2(OH)_4^{2-}$ (An = Np, Pu).[18−20] Lessons from the uranyl(VI) studies noted above suggest that, for hexavalent neptunyl(VI) ions, increasing alkalinity might shift the equilibrium from $NpO_2(OH)_4^{2-}$ to $NpO_2(OH)_5^{3-}$ and that alkaline solution environments might promote oxo-atom ligand exchange. In the present work, we extend our studies to the corresponding behavior of neptunium(VI) under similar environments and offer new evidence for oxo ligand exchange between neptunyl(VI) oxygen and water oxygen.

RESULTS AND DISCUSSION

Synthesis and Physicochemical Properties. In alkaline MOH solutions (M = Li, Na, K, Cs, NH_4), the UO_2^{2+} ion has a pervasive tendency to form highly insoluble alkali-metal uranate salts such as M_2UO_4 and $M_2U_2O_7$.[21] In previous studies of the UO_2^{2+} ion, we and others were able to avoid precipitation through the use of tetramethylammonium hydroxide [TMA(OH)] to maintain soluble uranyl species.[8,22] In the present study, we find that the NpO_2^{2+} ion exhibits reasonable solubility (0.05 M) over a range of alkalinity spanning 1−3.5 M MOH (M = Li, Na, TMA), producing light-pink solutions. In our synthetic preparations, we employed a 1 M nitric acid stock solution of known neptunium(VI) concentration. Aliquots of the neptunium(VI) stock solution were added directly to a stirring 3.5 M (TMA)OH solution, taking into account neutralization of the acid. The subsequent addition of $Co(NH_3)_6Cl_3$ to this stirred solution resulted in the deposition of small orange crystals of formula $[Co(NH_3)_6]_2[NpO_2(OH)_4]_3{\cdot}H_2O$ after 12 h of cooling to 5 °C.

Solid-State and Solution Molecular Structures. *Single-Crystal X-ray Diffraction.* Single crystals of $[Co(NH_3)_6]_2[NpO_2(OH)_4]_3{\cdot}H_2O$ that were suitable for X-ray diffraction analysis were prepared by cooling a dilute solution of $Co(NH_3)_6Cl_3$ (0.01 M) and neptunium(VI) (0.008 M) in 3.5 M (TMA)OH to 5 °C. The data collection and crystallographic parameters are summarized in Table 1, and selected bond lengths and angles are given in Table 2. A thermal ellipsoid drawing of the repeating unit containing the atom numbering scheme used in the tables is shown in Figure 1.

The asymmetric unit contains three distinct $NpO_2(OH)_4^{2-}$ ions, each displaying a pseudooctahedral coordination geometry with two *trans*-oxo ligands and four hydroxide ligands occupying coordination sites in an equatorial plane. The three independent $NpO_2(OH)_4^{2-}$ molecules in the unit cell give an average Np=O distance of 1.80(1) Å, with a range from 1.789(11) to 1.819(8) Å. The trans O=Np=O angle is 180.0°, while the cis O=Np−OH angle displays a narrow average of 90.2(1)°, with values ranging less than 4° from the idealized 90°. The average Np=O distance of 1.80(1) Å can be compared to the average Np=O distances of 1.731(18), 1.733(5), 1.736(18), 1.739(10), and 1.744(1) Å observed in solid-state structures of $NpO_2(NO_3)_3^-$,[23] $NpO_2Cl_4^{2-}$,[24] $NpO_2(OPPh_3)_2Cl_2$,[25] $NpO_2(OPPh_3)_2(NO_3)_2$,[25] and $NpO_2(H_2O)_5^{2+}$,[26] respectively. All of these complexes contain relatively weak equatorial donor ligands. The average Np=O distance of 1.80(1) Å is much closer to those that contain strong equatorial donor ligands and can be compared to 1.80(1), 1.776(7), and 1.774(3) Å, reported for solid-state structures of $NpO_2F_5^{3-}$,[27] $NpO_2(O_2CMe)_3^-$[23] and $NpO_2(CO_3)_3^{4-}$, respectively.[28] This general characteristic of a relatively long axial An=O bond is shared by the isostructural

Table 1. Summary of the Crystallographic Data for $[Co(NH_3)_6]_2[NpO_2(OH)_4]_3{\cdot}H_2O$

empirical formula	$H_{50}N_{12}O_{19}Co_2Np_3$
fw	1351.4
cryst syst	monoclinic
space group	$C2/c$
unit cell dimens	
a, Å	17.344(4)
b, Å	12.177(3)
c, Å	15.273(5)
β, deg	120.17(2)
V, Å^3	2788.7(13)
Z, molecules/cell	4
D_{calc}, g cm^{-3}	3.219
μ, mm^{-1}	12.336
λ(Mo Kα), Å	0.71073
temp, °C	293
measd reflns	2998
unique intens	2456
R1	0.0359
wR2	0.0729
GOF	1.047

Table 2. Selected Bond Distances (Å) and Angles (deg) for $[Co(NH_3)_6]_2[NpO_2(OH)_4]_3{\cdot}H_2O$

Np(1)−O(1)	1.790(11)	Np(2)−O(6)	2.245(8)
Np(1)−O(2)	1.789(11)	Np(2)−O(7)	2.215(9)
Np(1)−O(3)	2.254(7)	Np(3)−O(8)	1.802(8)
Np(1)−O(4)	2.277(8)	Np(3)−O(9)	2.213(9)
Np(2)−O(5)	1.819(8)	Np(3)−O(10)	2.262(9)
Co−N(1)	1.983(9)	Co−N(4)	1.970(9)
Co−N(2)	1.972(9)	Co−N(5)	1.974(9)
Co−N(3)	1.980(9)	Co−N(6)	1.984(9)
O(1)−Np(1)−O(2)	180.00(1)	O(5)−Np(2)−O(7A)	93.9(3)
O(1)−Np(1)−O(3)	87.9(2)	O(8)−Np(3)−O(8A)	180.00
O(1)−Np(1)−O(4)	90.6(2)	O(8)−Np(3)−O(9)	93.9(3)
O(5)−Np(2)−O(5A)	180.00	O(8)−Np(3)−O(9A)	86.1(3)
O(5)−Np(2)−O(6)	87.8(3)	O(8)−Np(3)−O(10)	88.2(3)
O(5)−Np(2)−O(6A)	92.2(3)	O(8)−Np(3)−O(10A)	91.8(3)
O(5)−Np(2)−O(7)	86.1(3)	O(9)−Np(3)−O(10)	89.8(3)

dx.doi.org/10.1021/ic3020139 | Inorg. Chem. 2013, 52, 3547−3555

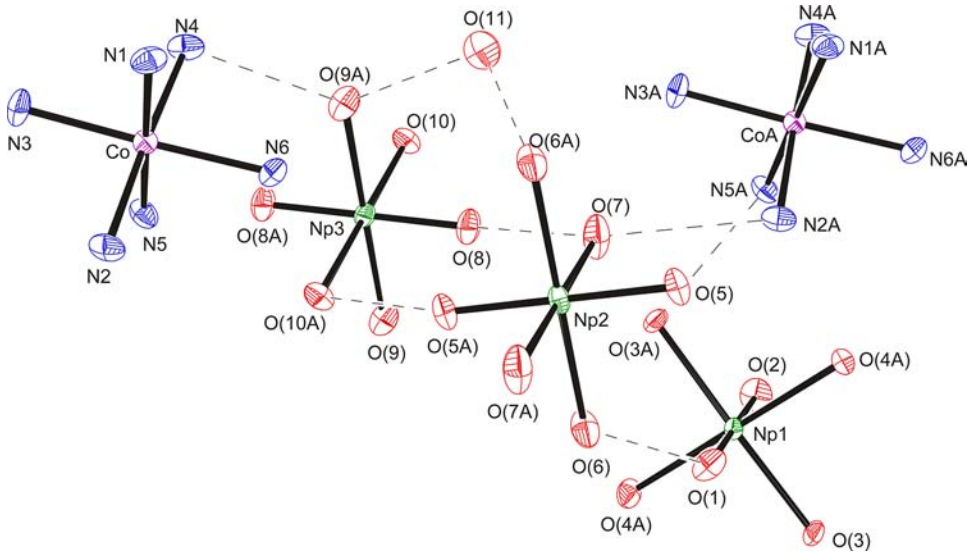

Figure 1. Thermal ellipsoid drawing of the repeating unit of $[Co(NH_3)_6]_2[NpO_2(OH)_4]_3 \cdot H_2O$ showing the atom labeling scheme used in the tables.

uranium analogue, $[Co(NH_3)_6]_2[UO_2(OH)_4]_3 \cdot H_2O$, whose average U═O distance of 1.82(1) Å[8] is also unusually long.

All of the oxo ligands of the three independent $NpO_2(OH)_4^{2-}$ ions have close contacts to oxygen atoms from OH^- ligands on neighboring neptunium units [average O···O = 2.768(6) Å] or NH_3 ligands from adjacent $Co(NH_3)_6^{3+}$ units [average O···N = 3.126(6) Å]. These distances are well within the range expected for weak hydrogen-bonding interactions.[29] In addition, some OH^- ligands have close contacts to a lattice H_2O molecule [average O···O = 2.851(6) Å] or $Co(NH_3)_6^{3+}$ ions [average O···N = 3.019(7) Å]. The average terminal Np−OH distance is 2.24(2) Å, with values spanning a relatively narrow range of 2.213(8)−2.277(8) Å. To the best of our knowledge, there are no similar terminal neptunium(VI) hydroxide structures available for comparison. Analogies may be made to the fluoro system $NpO_2F_5^{3-}$, where the average equatorial Np−F distance was found to be 2.26(1) Å,[27] which is similar to the Np−OH distance of 2.24(2) Å. The Np−OH distance is also similar to that found for the uranium analogue, which showed an average U−OH distance of 2.26(2) Å.[8]

The $Co(NH_3)_6^{3+}$ unit is pseudooctahedral and displays metrical parameters in the normal ranges, with an average Co−N distance of 1.977(9) Å.

X-ray Absorption Fine Structure (XAFS) Studies. X-ray absorption measurements were performed at the Np L_{III}-edge on single crystals of $[Co(NH_3)_6]_2[NpO_2(OH)_4]_3 \cdot H_2O$ in the solid state and on two alkaline solutions containing 0.05 M neptunium(VI) in either 2.5 or 3.5 M (TMA)OH. The crystalline solid of known stoichiometry served as a standard for background subtraction and curve-fitting parameters for determination of the coordination numbers in solution.

The background-subtracted k^3-weighted $\chi(k)$ and $\chi(R)$ for all three samples are very similar, and therefore only a representative set of spectra are shown here (see the Supporting Information). The background-subtracted k^3-weighted XAFS spectrum of 0.05 M neptunium(VI) in a 3.5 M (TMA)OH solution is provided in Figure 2 (inset), where experimental data are shown as a red line and the theoretical fit is indicated as a blue line. The Fourier transform (FT) modulus

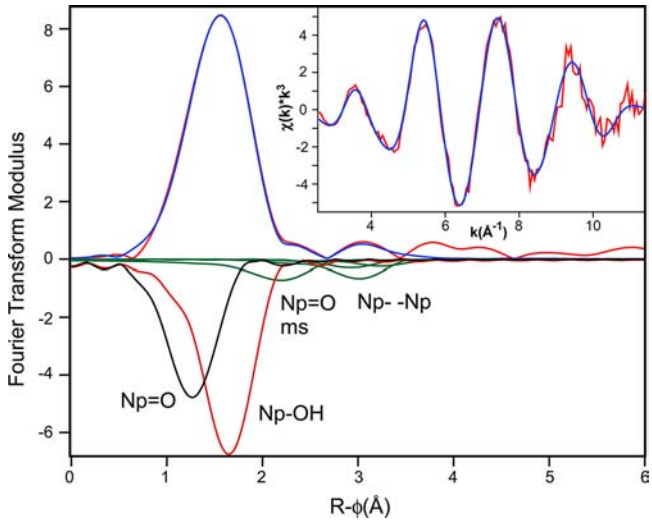

Figure 2. FT (without phase corrections) of the k^3-weighted EXAFS spectrum of neptunium(VI) in 3.5 M (TMA)OH. The red line is the experimental data, and the blue line is the theoretical fit. Shown with negative FT amplitudes are the individual contributions of the oxo and equatorial shells, O═Np═O multiple scattering, and Np---Np backscattering paths to the fit. The contributions of these last two can be seen to be negligible compared to the noise level projected from the features at high *R*. Inset: Background-subtracted k^3-weighted EXAFS spectra (red) and fit (blue) of 3.5 M (TMA)OH neptunium(VI) solutions.

and theoretical fit (without phase corrections) of the k^3-weighted data are shown in Figure 2. Note that, because the FT is not corrected for the XAFS phase shift, the peak positions are 0.2−0.5 Å lower than the actual Np−O distances.[30,31] A comparison of both $\chi(k)$ and $\chi(R)$ representations of the spectra indicates good fits in both phase and amplitude for this spectrum and equivalent correspondence between the data and fit for the solid-state and other solution samples (not shown).

The theoretical XAFS modeling code, FEFF7 of Rehr et al.,[30,31] was used to calculate the backscattering phases and amplitudes of the individual neighboring atoms, using symmetrical model structures. A summary of the XAFS structural

dx.doi.org/10.1021/ic3020139 | *Inorg. Chem.* 2013, 52, 3547−3555

and fitting parameters for the solid and both solutions is given in Table 3. The curve fitting reveals that the asymmetric peak in the FT spectra (Figure 2) contains the overlapping contributions from both the axial oxo and equatorial OH shells whose small separation in Np−O distance generates a single broad peak over this transform range. Because the coordination number is highly correlated with both the amplitude (S_0^2) and Debye−Waller (σ^2) factors, certain constraints were placed on the fitting.

Table 3. Summary of EXAFS Results for Neptunium(VI) in 2.5 and 3.5 M (TMA)OH Solution and in $[Co(NH_3)_6]_2[NpO_2(OH)_4]_3{\cdot}H_2O$[a]

shell	R (Å)	n	σ (Å)	ΔE^0 (eV)	SF
Solid $[Co(NH_3)_6]_2[NpO_2(OH)_4]_3{\cdot}H_2O$					
Np=O	1.82(1)	2.0*	0.074	7.5	1.06
Np−O	2.23(1)	4.0*	0.084	5.5	1.16
2.5 M (TMA)OH Solution					
Np=O	1.80(1)	2.0	0.074*	2.50	1.06*
Np−O	2.23(1)	3.8	0.094	0.76	1.16*
3.5 M (TMA)OH Solution					
Np=O	1.80(1)	1.8	0.074*	2.5	1.06*
Np−O	2.22(1)	5.5	0.096	1.5	1.16*

[a]Data were fit to χk^3 from k = 3.00 to 11.3, 13.5, and 12.6, respectively. Values with asterisks were fixed.

For the crystalline solid of known composition $[Co(NH_3)_6]_2[NpO_2(OH)_4]_3{\cdot}H_2O$, the data were fit by fixing the coordination numbers of both the first and second shells at the known values of 2.0 axial and 4.0 equatorial oxygen atoms, respectively. The other parameters were allowed to float with the constraint that the S_0^2 values for both shells were required to be within 0.1 units and the ΔE_0 values for both shells to be within 2 eV of each other. The resulting Np=O and Np−OH distances were found to be 1.82(1) and 2.23(1) Å, respectively, which correspond adequately with the average values of 1.80(1) and 2.24(1) Å found in the single-crystal X-ray structure. The other parameters, σ, ΔE_0, and S_0^2, were within reasonable limits (Table 3).

The data for the two solution samples were subsequently fit utilizing some of the parameters determined for the solid standard. Most important for accurate coordination numbers, the amplitude factors (S_0^2) for the first two shells were fixed to those determined for the solid. For the sample of neptunium(VI) in 2.5 M (TMA)OH, the best fits to the first and second shells revealed 2.0 and 3.8 oxygen atoms, respectively, at distances of 1.80(1) and 2.23(1) Å, suggesting an average molecular stoichiometry of $NpO_2(OH)_4^{2-}$ as found in the solid state. In comparison, the best fits to the data obtained for neptunium(VI) in a 3.5 M (TMA)OH solution revealed two shells consisting of 1.8 oxygen atoms at a distance of 1.80(1) Å and 5.5 oxygen atoms at 2.22(1) Å, consistent with an average stoichiometry of $NpO_2(OH)_5^{3-}$.

Over the past decade, numerous XAFS studies of uranyl(VI) ions have been reported,[32−34] where the data analyses required inclusion of an O=U=O multiple scattering pathway with an effective R value twice that of the U=O distance. In $UO_2(CO_3)_3^{4-}$, for example, this pathway was calculated to have an amplitude of ca. 21% of the single U=O scattering path.[33] Inclusion of an O=Np=O multiple scattering pathway does improve the fits but only marginally. In addition to the lack of a significant multiple scattering pathway, no evidence of a Np---Np backscattering interaction expected for polymeric species was found, consistent with maintenance of a monomeric species in solution. The contributions of these two waves that are well separated from the first coordination shells are shown in the figure; the magnitudes and improvements to the fit are negligible relative to the low noise level observed at high R. The results were therefore not included in the table.

From the XAFS structural parameters (Table 3), several features are apparent. First, we are struck by the essentially identical axial [Np=O = 1.80(1) Å] and equatorial [Np−OH = 2.22(1) and 2.23(1) Å] distances derived for both solution samples, analogous to that found for uranyl analogues.[8] We also note that for the solid of known composition $NpO_2(OH)_4^{2-}$ our axial Np=O bond lengths from EXAFS and X-ray diffraction differ by 0.02 Å, indicating the lower accuracy of our EXAFS data. Finally, we note an apparent increase in the average number of OH^- ligands bound to the neptunium atom in the 3.5 M (TMA)OH solution relative to either the 2.5 M (TMA)OH solution or the $[Co(NH_3)_6]_2[NpO_2(OH)_4]_3{\cdot}H_2O$ solid (which give the same numbers of oxygen atoms within our level of uncertainty). This behavior is consistent with that observed in the analogous uranium(VI) system, where it is now accepted that there is an equilibrium between the tetra- and pentahydroxo complexes,[8,12] and suggests that a similar equilibrium may be active for neptunium(VI) in a (TMA)OH solution under the conditions presented here (eq 1).

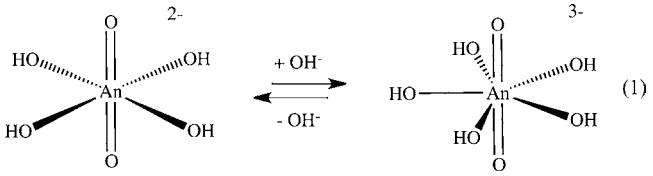

(1)

XAFS Evaluation of the Number of Equatorial Ligands. Advances in the theory of X-ray absorption have led to the widespread development and application of theoretical modeling codes such as FEFF.[31,35] These powerful computational codes do an outstanding job of calculating the theoretical phases and amplitudes of known structures, and such calculated parameters are commonly employed as initial fitting parameters to fit unknown structures. The application of FEFF to our neptunyl hydroxide data suggests an increase in the number of equatorial ligands with increasing hydroxide concentration. Recall that EXAFS studies of the related uranium(VI) system by different researchers under different solution conditions generated controversy over the number of OH^- ligands prior to NMR confirmation that the system was an equilibrium mixture of $UO_2(OH)_4^{2-}$ and $UO_2(OH)_5^{3-}$.[8] Prior to the advent of these powerful theoretical XAFS modeling codes, the historical approach to determining the coordination number from XAFS was to employ standard compounds of known stoichiometry and extract the phase and amplitude functions directly for comparison with the unknown sample. In order to gain more insight in our assessment of a potential change in the equatorial coordination number with the (TMA)OH concentration, we examined the known solid of formula $[Co(NH_3)_6]_2[NpO_2(OH)_4]_3{\cdot}H_2O$, where fits employing FEFF phases and amplitudes produced a result of four equatorial OH^- ligands. We then employed this known compound to extract experimental amplitude functions for comparison with solutions using the ratio method. In this method, the data are

dx.doi.org/10.1021/ic3020139 | Inorg. Chem. 2013, 52, 3547−3555

Fourier-transformed, and the shell of interest is isolated and then back-transformed to provide an individual wave or amplitude function. This procedure eliminates information on the phase factors and allows the amplitudes to be compared directly.[36,37] While this approach is somewhat dated in light of the current theoretical capability, the approach was originally developed for ratioing known and unknown amplitude functions, and we have found that it still has great utility and some unique advantages. First, although calculated amplitudes and phases are quite accurate, they still do not include all chemical effects that can diminish the accuracy of the results but that are eliminated as a source of error in the direct comparison of spectra from two closely related compounds. More importantly, instead of giving a single value, a ratio allows the data to be inspected over its full range and compared against the expected functional forms, i.e., a horizontal line for amplitudes. It therefore identifies errors in the data that are approximately compensated for by the floating parameters in the fit and also provides a direct means for generating a true error in the calculated value by the standard deviation from the correction functional form.

Figure 3 shows the plots of the amplitudes of the isolated waves from the axial oxo and equatorial hydroxide shells of the

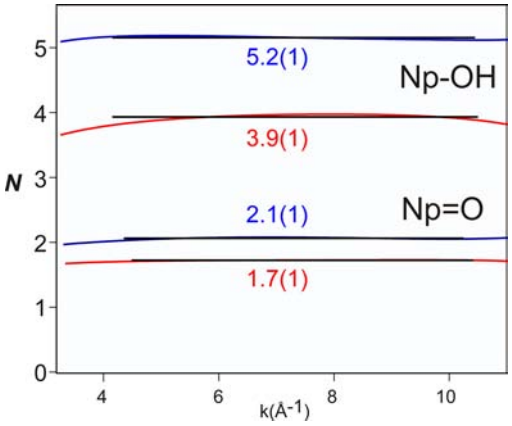

Figure 3. Amplitudes for the individual axial Np=O and equatorial Np−OH EXAFS shells from neptunium(VI) in 2.5 M (blue) and 3.5 M (red) (TMA)OH solutions, divided by the same amplitudes from the crystalline $NpO_2(OH)_4^{2-}$ standard.

solutions ratioed against those of the crystalline standard. As can be seen, the average coordination number for the first shell of oxo atoms in both solution samples was 2.0 (±0.2). In addition, for the comparison between the second shell of hydroxides, the ratio or average OH coordination number in the 3.5 M (TMA)OH solution is 20−25% larger than that in 2.5 M (TMA)OH over the entire data range, with both results giving close to integer values. Furthermore, all of the results are quite close to the expected horizontal line, demonstrating that the data and the application of the technique are both high quality. This analysis supports the hypothesis that the average OH^- coordination number increases in the more strongly alkaline solution and suggests a predominance of $NpO_2(OH)_4^{2-}$ at lower hydroxide concentration, with an increase to some amount of $NpO_2(OH)_5^{3-}$ with higher hydroxide concentration.

Spectroscopic Studies. *Vibrational Spectroscopy and Evidence for Oxo Ligand Exchange.* A Raman spectroscopic study was performed on alkaline solutions of neptunium(VI) along with single crystals of $[Co(NH_3)_6]_2[NpO_2(OH)_4]_3{\cdot}H_2O$ to probe the symmetric ν_1(O=Np=O) stretch for evidence of more than one species in solution and for evidence of oxo ligand exchange. The presence of a strong Raman-active band for Me_4N^+ at 762 cm^{-1} precluded conducting the solution studies in (TMA)OH.

Solution Raman Spectroscopy. The neptunyl(VI) Raman spectra were studied for 0.05 M NpO_2^{2+} in 0.6−2.2 M LiOH solutions under a constant ionic strength of 2.2 M (maintained through the addition of $LiNO_3$), and all samples revealed a single peak at 769 cm^{-1}, indicating a single detectable neptunyl(VI) solution species by Raman spectroscopy at room temperature. A representative solution Raman spectrum is shown in Figure 4.

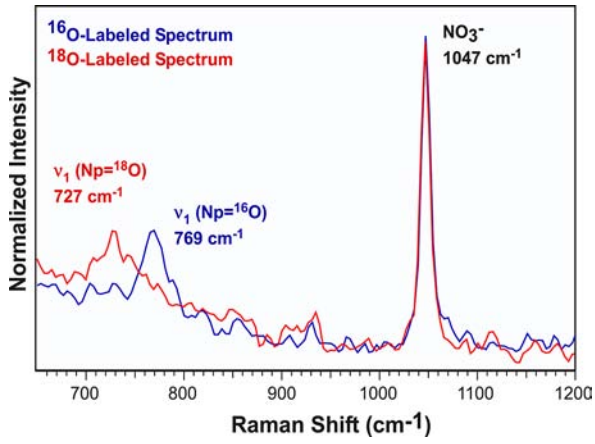

Figure 4. Raman spectrum of 0.05 M $[NpO_2]^{2+}$ in 2.2 M LiOH (blue). The ^{18}O-labeled Raman spectra (red) from the mixing of ^{18}O-enriched H_2O with the evaporate and subsequent incorporation of ^{18}O into the dioxo moiety.

The presence of a second species, as inferred from XAFS data, cannot be discounted because the relative cross sections for each of the species are unknown. The ν_1 frequency of 769 cm^{-1} represents an 87 cm^{-1} shift to lower energy relative to that observed (856 cm^{-1}) for the neptunium(VI) aquo ion $NpO_2(H_2O)_5^{2+}$ in a perchloric acid solution.[38] The shift to lower energy is consistent with the longer Np=O bond found in the hydroxide system. For large molecules, isotopic substitution is indispensable in making band assignments because only vibrations involving the motion of the isotopic atom will be shifted by isotopic substitution. If the 769 cm^{-1} feature observed in the neptunium(VI) solution is the ν_1(O=Np=O) stretching mode, then isotopic substitution of the oxo ligands with 98% ^{18}O should produce a 6% shift in the ν_1 vibration to lower frequency, equivalent to the square root of the ratio of the atomic masses according to the Redlich−Teller product rule.[39] Neptunium(VI) in a 1 M HCl solution was dissolved into a natural-abundance 2.5 M LiOH solution, taking into account the neutralization of acid. After removal of an aliquot for Raman analysis, the solution was evaporated to dryness under vacuum. The resulting residue was subsequently dissolved in 98% ^{18}O-enriched $H_2{}^{18}O$ to give an alkaline $Li^{18}OH$ solution of the same volume. Raman measurements were performed on both solutions. The natural-abundance sample showed the expected single ν_1 peak at 769 cm^{-1}. The Raman spectrum for the ^{18}O-enriched sample showed a single ν_1 stretch at 727 cm^{-1} (Figure 4). The shift in the stretching

dx.doi.org/10.1021/ic3020139 | Inorg. Chem. 2013, 52, 3547−3555

frequency (42 cm^{-1}) is only slightly less than the theoretical 46 cm^{-1} (6%) shift expected from the isotope mass effect on an isolated $[O{=}Np{=}O]^{2+}$ moiety. Thus, isotopic substitution identifies the 769 cm^{-1} peak as the ν_1 symmetric stretch of the O═Np═O moiety.

The rapid exchange and relative ease of ^{18}O isotopic substitution in a LiOH solution is remarkable. The time required to remove natural-abundance H_2O in vacuo, redissolve in 98% $H_2{}^{18}O$, and then record the Raman spectrum was approximately 2 h. The Raman spectrum revealed a new ν_1 stretch at 727 cm^{-1}, with no detectable peak at 769 cm^{-1} (Figure 4) meaning that the exchange was nearly complete on this time scale. Moreover, upon reversing the process to remove $H_2{}^{18}O$ in vacuo and redissolving in natural-abundance H_2O, one observes the reappearance of the peak at 769 cm^{-1}, indicating that the process is chemically reversible. In contrast, under perchloric acid conditions, the 856 cm^{-1} ν_1 stretching frequency for the $NpO_2(H_2O)_5^{2+}$ ion remains invariant in the presence of $H_2{}^{18}O$ during a similar time frame. Oxo ligand exchange will occur in an acid solution, but Rabideau has shown that the half-life is ≥19 days, with an oxo ligand exchange rate of $\leq 6 \times 10^{-7}$ s.[40] The ability to completely exchange the oxo ligand in only a few hours represents a significant increase in the relative exchange rate.

Solid-State Raman Spectroscopy. The Raman spectrum of single crystals of $[Co(NH_3)_6]_2[NpO_2(OH)_4]_3{\cdot}H_2O$, where the molecular species $NpO_2(OH)_4^{2-}$ is known definitively, reveals a ν_1 frequency at 742 cm^{-1}. The 27 cm^{-1} difference between solution and solid-state frequencies is significant, and larger than expected for matrix (i.e., solution vs solid state) conditions. To confirm the identity of this peak as the ν_1 symmetric stretch, we employed isotopic substitution, where single crystals of $[Co(NH_3)_6]_2[NpO_2(OH)_4]_3{\cdot}H_2O$ were grown from 98% ^{18}O-enriched solutions. The Raman spectrum of this ^{18}O-enriched sample revealed a ν_1 stretch at 701 cm^{-1}, whose 40 cm^{-1} shift is very close to the theoretical 6% shift of 44 cm^{-1}. This definitively identifies the 742 cm^{-1} frequency as the ν_1 symmetric stretch in the solid containing the $NpO_2(OH)_4^{2-}$ ion. We note that the isotopic substitution is nearly complete, providing additional evidence for a rapid oxo ligand exchange with enriched solvent water. With multiple crystallization attempts from a (TMA)OH solution, occasionally crystalline mixtures of two morphologies (needles and plates) were obtained. The Raman spectrum of the crystalline mixture revealed a strong peak at 741 cm^{-1} and a higher-frequency peak of weaker intensity at 768 cm^{-1}. This spectrum is shown in Figure 5. The predominant 741 cm^{-1} peak coincides with that seen in pure crystals containing the $NpO_2(OH)_4^{2-}$ ion (742 cm^{-1}). The minor peak at 768 cm^{-1} is coincident with that observed in solution (769 cm^{-1}).

The relatively low ν_1 observed for the solid containing $NpO_2(OH)_4^{2-}$ is unexpected when compared to the solution samples. The sensitivity of the ν_1 Raman mode to the number of equatorial ligands in uranyl(VI) complexes is well-known.[41] In general, one observes a decrease in ν_1 with each successive ligand added to the system. On the basis of these Raman scattering properties,[8] one would anticipate that $NpO_2(OH)_4^{2-}$ would have a higher ν_1 frequency than $NpO_2(OH)_5^{3-}$. In the case of the $UO_2(OH)_n^{2-n}$ system, the solid containing $UO_2(OH)_4^{2-}$ exhibited a ν_1 frequency at 796 cm^{-1}, and solutions revealed a single lower energy ν_1 at 786 cm^{-1}.[8] The equilibrium constant for the equilibrium between $UO_2(OH)_4^{2-}$ and $UO_2(OH)_5^{3-}$ (eq 1) was determined by Szabo and Grenthe[12] and Moll et al.[22] to be between 0.1 and 0.01, meaning that the uranium solutions on which Raman data were collected contained predominantly $UO_2(OH)_4^{2-}$, with only a small amount of $UO_2(OH)_5^{3-}$, and that the 10 cm^{-1} shift between the solid and solution is likely a matrix effect. The 27 cm^{-1} difference between solution and solid-state frequencies in the case of neptunium(VI) may be also be due to matrix effects, but other possibilities should also be considered. For neptunium(VI), the f-electron manifold is now populated, and known low-lying electronic states based on f–f transitions[42−46] may affect the observed vibrational frequencies. We note that for six-coordinate $NpO_2Cl_4^{2-}$ the (f,f) electronic states include a low-lying a_{1g} electronic state at ∼1000 cm^{-1}, which is of the same symmetry as the a_{1g} ν_1 dioxo vibration.[42,45,46] Coupling could result in a change of the vibrational state energy, thereby altering the observed ν_1 frequency. Further studies would be needed to assess such a mechanism. Without such data, we are forced to conclude that the most likely reason for the difference between solid and solution is a matrix effect.

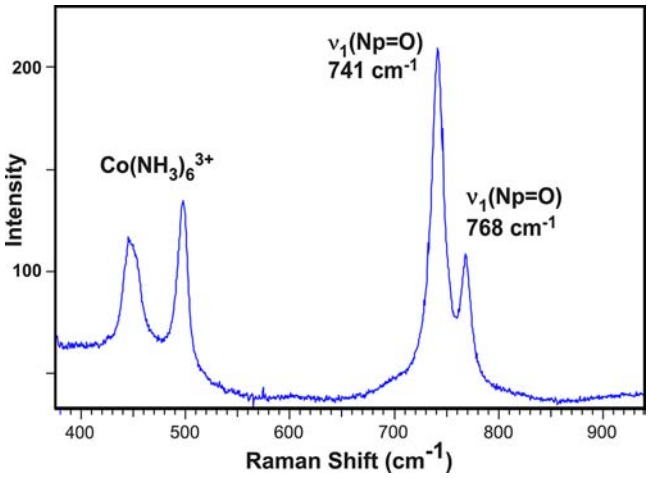

Figure 5. Raman spectra of cobalt hexamine crystals that show both peaks at 741 and 768 cm^{-1}. Peaks at 445 and 499 cm^{-1} are from the $Co(NH_3)_6^{3+}$ ion.

^{17}O NMR Studies. One of the unique properties observed for uranium(VI) under highly alkaline solution conditions is a ligand-exchange process that exchanges the oxygen atoms of the oxo ligands with the oxygen atoms of the H_2O/OH^- solvent system. This process is unusual in view of the well-known chemical inertness of the UO_2^{2+} oxo ligands under acidic and neutral conditions but has been confirmed by our group, Grenthe et al., and Moll et al. employing ^{17}O NMR[8,12,22] and ^{18}O Raman[8] spectroscopy, for uranium(VI) in both NaOH and TMAOH solutions. Appelman et al.[47] attempted to study the neptunium(VI) oxo ligand exchange in alkaline solution but could not observe a ^{17}O NMR signal for the neptunium(VI) oxo atoms and attributed the lack of signal to a combination of paramagnetism (f^1) and oxo group ligand-exchange processes.[47] We have confirmed that result by monitoring a fully 4% ^{17}O-enriched solution of neptunium(VI) in 3.5 M (TMA)OH. As in the Appelman et al. study, no peak was observed for the oxo ligands despite the fact that we can easily observe an ^{17}O NMR resonance at δ 2899 for a 0.07 M sample of NpO_2^{2+} in 1 M $HClO_4$. The observation of a distinct ^{17}O signal in an acid solution where oxo ligand exchange is known to be slow suggests that the lack of a signal in alkaline solution

dx.doi.org/10.1021/ic3020139 | *Inorg. Chem.* 2013, 52, 3547−3555

is more likely due to an exchange process that is comparable to the time scale of the NMR experiment, effectively "washing out" the signal in the baseline.

DISCUSSION

The single-crystal X-ray diffraction study definitively identifies the presence of the $NpO_2(OH)_4^{2-}$ ion in the solid state. The EXAFS data in the solid state and both solutions give essentially identical Np=O and Np−OH bond lengths but with differences in the equatorial coordination number. EXAFS-derived bond lengths are generally quite reliable, but extracting accurate coordination numbers has often been controversial. We devoted a good deal of effort to evaluating potential coordination number changes from our EXAFS data that suggest an increase in the coordination number, but the fact that the bond lengths are nearly identical in all three samples is inconsistent with an increase in the equatorial coordination number. It is well established that an increase in the equatorial coordination number is generally accompanied by an increase in the bond length of the equatorial ligand.[21] There are always cases where the expected change is very small, such as the case of $UO_2Cl_4^{2-}$ and $UO_2Cl_2(THF)_3$, where an increase in coordination is only accompanied by a 0.02 Å change in the equatorial U−Cl distance [2.67(1) and 2.69(2) Å],[48,49] but there is also a change in molecular charge.

The Raman spectra for solid and solution show differences in ν_1, suggesting that there may be different species present in solid and solution. However, the direction of the shift goes against conventional wisdom.[41] An increase in the equatorial coordination number is generally accompanied by a decrease in the axial ν_1(O=Np=O), and our observed shift between solid and solution data goes in the opposite direction. So, the Raman shift is not consistent with a coordination number change but is more likely associated with a matrix effect, or even vibrational−electronic coupling. If the Raman shift between solid and solution is due to effects other than the coordination number, then it is possible that the predominant species in solution is simply $NpO_2(OH)_4^{2-}$. This would reconcile both bond-length and vibrational-frequency observations. Such a conclusion is consistent with the data amassed over the past decade for the corresponding uranium analogue. For uranium, it is now established that both $UO_2(OH)_4^{2-}$ and $UO_2(OH)_5^{3-}$ exist in solution but that at room temperature, under conditions similar to those studied here, the predominant solution species is $UO_2(OH)_4^{2-}$. If the similarity holds for neptunium, then the Raman shift from $AnO_2(H_2O)_5^{2+}$ to $AnO_2(OH)_4^{2-}$ is very similar for both uranium (74 cm^{-1}) and neptunium (87 cm^{-1}). Both Moll and Szabo noted an equilibrium constant between 0.1 and 0.01,[12,22] making $UO_2(OH)_4^{2-}$ the predominant solution species, and they noted the appearance of an additional peak in the ^{17}O NMR spectrum at higher (TMA)OH concentrations, consistent with the ingrowth of $UO_2(OH)_5^{3-}$. This would be in agreement with the observed increase in the coordination number with increasing (TMA)OH for the neptunium system but perhaps not as dramatic as that suggested by the EXAFS data. This would also be consistent with solution conditions studied for $AnO_2(OH)_4^{2-}$ (uranium, neptunium, and plutonium) by a number of groups.[12,18] We conclude, therefore, that our data are most consistent with the presence of $NpO_2(OH)_4^{2-}$ as the predominant species in solution under both (TMA)OH concentrations. It is likely that a small amount of $NpO_2(OH)_5^{3-}$ grows in with increasing alkalinity. We look forward to further studies in this area.

EXPERIMENTAL SECTION

General Considerations. All operations were carried out inside HEPA-filtered fume hoods or negative-pressure gloveboxes designed for containment of radioactive materials. Standard radiochemical procedures were used throughout. $Co(NH_3)_6Cl_3$, NaOH (Aldrich), LiOH (Baker), and $Me_4N(OH)$ (Fisher) were all used as received. ^{17}O-enriched H_2O (20%) and ^{18}O-enriched H_2O (98%) were obtained from Los Alamos National Laboratory stock and used without further purification. NMR spectra were recorded on a Bruker AMX500 spectrometer with a 5 mm broad-band probe operating at 67.8 MHz (^{17}O) with a ^2H field-frequency lock; the peak positions are reported with positive shifts downfield of external H_2O set at δ = 0.0 ppm. The temperature was controlled with a Bruker variable-temperature controller and was stable to within ±1 K. The temperature was determined by measurement of the ^1H NMR spectra of ethylene glycol (295−350 K). For each ^{17}O NMR sample, the solution was transferred to a 4-mm-o.d. Teflon FEP NMR tube insert (Wilmad), which was subsequently sealed using either a polyethylene plug or heat from a small soldering gun. The Teflon insert was then transferred to a standard 5-mm-o.d. glass NMR tube. Raman vibrational spectra were obtained by excitation in the near-IR obtained using an argon-pumped titanium-sapphire continuous-wave (CW) laser (752 nm, Spectra Physics model 3900s). The Raman scattering was dispersed with a single-stage monochromator (diffraction gratings blazed at 1150 nm; 4 cm^{-1} resolution), after being prefiltered through an interference filter designed to remove Rayleigh scattered laser light, to a CCD detector (Princeton Instruments). An alternative Raman vibrational spectroscopic method entailed the use of a FT Raman spectrometer (Nicolet Raman 960 ESP attachment to the Magna-IR 560 FT-IR spectrometer). The sample was irradiated with ∼0.4 W from an air-cooled diode-pumped Nd:YVO_4 CW laser operating at 1064 nm, and the scattered light was collected with 180° collection optics and relayed to the FT-IR interferometer. The interferometer was equipped with an extended XT-KBr beamsplitter and an InGaAs detector. Spectra were collected at 8 cm^{-1} resolution and signal-averaged over 1024 scans. The Raman samples were recorded in sealed 5 mm glass NMR tubes.

Acquisition and Analysis of XAFS Spectra. Np L_{III} XAFS spectra were measured at the Stanford Synchrotron Radiation Laboratory, under dedicated operating conditions (3.0 GeV, 50−100 mA), on end station 4-2 (unfocused). Solution samples were measured at ambient temperature. The EXAFS sample cells were designed to enable EXAFS studies of radioactive materials at a nonnuclear facility. The primary sample cell consisted of a Teflon body with a Kapton (high-strength polyimide film, DuPont) window, which had been pressure tested to 28.8 psi. The sample was loaded and tested for contamination and placed inside a secondary container of the same design, which was subsequently placed inside a third container with Kapton windows and mounted inside the X-ray experimental hutch. The experimental hutch was modified for radiochemical experiments using a portable experimental enclosure within the hutch. This allowed for maintenance of three zones of negative pressure, and the vacuum system passed through 0.3 μm HEPA filters. The hutch was equipped with continuous air monitors and radiation sampling safety equipment and monitored continuously throughout the course of the experiment.

Silicon [220] crystals were used to monochromate the beam. Harmonics were eliminated with a flat, platinum-coated mirror with a cutoff energy of 20−25 keV. All spectra were recorded in fluorescence mode. Fluorescence was measured with a multielement germanium detector, using analog or digital amplifiers and controlling the beam size and sample−detector distance to keep the count rates below 120 kHz for each channel. The signals from each detector element were combined after preliminary analysis and inspection, weighting based on the signal (counts across the edge): noise (square root of total counts). For fluorescence data, a dead-time type of correction was made to adjust the absorption peak height to match that of the transmission data when applicable. This can correct for self-absorption as well as dead time. Energy calibration was accomplished by measuring the spectrum of a zirconium foil before and after the scans

dx.doi.org/10.1021/ic3020139 | Inorg. Chem. 2013, 52, 3547−3555

of the samples. The first inflection point of the zirconium foil was defined as 17999.35 eV. Two scans were performed on the neptunium solution data and averaged after preliminary analysis and inspection. After the absorbance was calculated by dividing the corrected fluorescence counts by the incident intensity, it was normalized by offsetting it so that the value of a second-order polynomial fit through the preedge was zero and scaling it so that the value of a third-order polynomial fit through the region above the edge was unity at 18075 eV. The reported peak energies are the zeroes of the first derivative; the edge energies are the inflection points of the absorption edges. Differentiation was performed numerically. The precision of the results so obtained is much better than the ca. 0.8 eV interval between data points because it also depends on the much finer interval of the absorption data. The precision is thus derived from the accuracy of the energy determination and the error in the monochromator position. From our experience with duplicate samples, the accuracies of the tabulated energies are 0.2−0.5 eV or better, with higher errors occurring in comparisons of spectra collected in different runs and lower errors for spectra measured during the same run; i.e., there can be problems with poorly understood, systematic experimental errors that can affect these results. We note, however, that no conclusions described in this report are based on single results and that all of the trends identified and discussed are strictly monotonic.

The EXAFS was extracted from the spectra by using a polynomial spline function to approximate the smooth atomic absorption. This was optimized by minimizing the area of the FT modulus from 0 to 1.1 Å. Substantial effort was made to use the same polynomial spline parameters and obtain the same function for all spectra to minimize the effects of background artifacts on the curve-fitting results. Metrical results were obtained by curve fits of the $k^3\chi(k)$ data over the ranges depicted in the figures, which generally used the full spectral range available but are not identical for all samples. FTs were performed over the same range, also using k^3 weighting to enhance the accuracy for the oxygen shells and with sine windows. Curve fits were performed using the values and constraints discussed in the text and listed in the table. The data for the two neptunium(VI) solution samples were fit by utilizing some of the parameters determined for the solid standard. For both solutions, the data were fit by fixing the first shell σ value and the corresponding S_0^2 values for the first two shells to those determined for the solid. Other constraints utilized for the fits include the following: (1) the coordination numbers for the first two shells were constrained to be 2 ± 0.3 and 4 ± 1, respectively; (2) the ΔE_0 value for the first shell was constrained to be 5 ± 2.5 eV; (3) the ΔE_0 value for the second shell was required to be within 2 eV of the ΔE_0 value for the first shell.

The theoretical EXAFS modeling code, FEFF7, of Rehr et al.[31,35] was employed to calculate the backscattering phases and amplitudes of the individual neighboring atoms, using the structure of crystallographic, monomeric $NpO_2(OH)_4^{2-}$. Amplitude ratioing was performed by separating the individual components by subtracting the waves of the fit for all of the other shells except the one to be ratioed from the raw data and then proceeding as described in the text and reference.

Standard Preparation of Neptunium(VI) Stock Solution. Disks of neptunium carbide were dissolved in concentrated $HClO_4$ to produce a solution that contains a mixture of neptunium(V) and neptunium(VI) aquo species. A 5 mL aliquot of the $HClO_4$ solution was transferred to a 20 mL vial, and 10.7 M NaOH was slowly added to the rapidly stirring solution. ***Caution!*** *Rapid addition of the strong base to the strong acid solution can result in the superheating of the solution.* NaOH was added until a brown precipitate of $NpO_2(OH)_2$ appeared and the solution was colorless. The resulting suspension was transferred to a polycarbonate centrifuge tube and the solution subsequently centrifuged for 10 min at 5000 rpm. After the initial centrifugation, the solution was removed and the solid washed three times with H_2O, centrifuging between each washing. The resulting solid was dissolved in 5 mL of 1 M HNO_3. The oxidation state was adjusted by bubbling the solution with O_3 overnight. This procedure gave a solution with an approximate neptunium concentration of 0.3 M. The oxidation state purity and concentration was determined by monitoring the electronic absorption spectrum in 1 M $HClO_4$ ($\varepsilon_{1223\ nm}$ = 45 M^{-1} cm^{-1}).

Synthesis of $[Co(NH_3)_6]_2[NpO_2(OH)_4]\cdot H_2O$. To a stirring solution of NpO_2^{2+} (0.008M) in 3.5 M (TMA)OH was added a dilute solution of $Co(NH_3)_6Cl_3$ (0.01 M), and the resulting mixture was cooled to 5 °C. In essentially quantitative yield, small orange crystals of $[Co(NH_3)_6]_2[NpO_2(OH)_4]_3\cdot H_2O$ were deposited after cooling of the solution for 12 h at 5 °C. After removal of the mother liquor, the crystals were washed with MeOH. These crystals are slightly soluble in 3.5 M (TMA)OH. Reactions were typically performed in 5 mL of solution in a 20 mL scintillation vial.

Solution Preparations. *Preparation of Neptunium(VI) Samples for EXAFS Analysis.* An aliqout of a 0.3 M neptunium(VI) stock solution (0.167 mL) is dissolved in 0.833 mL of the desired base [2.2 M LiOH or 2.5 or 3.5 M (TMA)OH]. After centrifugation for 10 min at 5000 rpm, the pink solution was transferred to a 4-mm-o.d. Teflon tube and heat-sealed. The filled Teflon tube was mounted to the interior of an EXAFS sample holder, which was then subsequently doubly contained with Kapton film. ***Warning!*** *(TMA)OH is corrosive and will dissolve Kapton.*

Preparation of Neptunium(VI) Samples in 2.2 M LiOH for Raman Analysis. An aliqout of a 0.3 M neptunium(VI) stock solution (0.334 mL) was dissolved in 1.666 mL of 2.2 M LiOH. After centrifugation for 10 min at 5000 rpm, 0.3 mL of the pink solution was transferred to a 5 mm glass NMR tube. The remainder was saved for the labeling studies. Raman shift (cm^{-1}): 769.

Raman ^{18}O-Labeling Study. The remaining 1.7 mL of the neptunium(VI) solution was dried by warming (80 °C) the solution for 30 min. The resulting residue was redissolved in 1.7 mL of 98% enriched $H_2{}^{18}O$ and the Raman spectrum collected. Raman shift (cm^{-1}): 742.

^{17}O NMR Samples. The NMR samples were prepared using a 4% ^{17}O-enriched 3.5 M (TMA)OH solution obtained by dissolving (TMA)OH·$5H_2O$ in 20.4% enriched $H_2{}^{17}O$ and natural-abundance $H_2{}^{16}O$ in a 1:4 ratio. An aliquot of the neptunium(VI) stock solution (0.083 mL, 0.3 M Np) was added to the enriched (TMA)OH solution (0.907 mL) and D_2O (0.010 mL). The solution was centrifuged for 10 min at 5000 rpm and the resulting pink solution transferred to the NMR tube as described above.

X-ray Crystallography. An orange needle-shaped crystal of $[Co(NH_3)_6]_2[NpO_2(OH)_4]\cdot H_2O$ with dimensions 0.12 × 0.12 × 0.21 was mounted on a 0.2 mm capillary after being coated with epoxy. This capillary was transferred into another capillary, the end of which was sealed with epoxy. The final layer of containment consisted of dipping the outer capillary into Hard as Nails nail polish. The coated capillary was finally mounted in a metallic pin and transferred to the goniometer of a Siemens SMART diffractometer equipped with a CCD area detector. The lattice parameters were optimized from a least-squares calculation on 25 carefully centered reflections of high Bragg angle. The data were collected using ω scans with a 0.86° scan range. Three check reflections monitored every 97 reflections showed no systematic variation of the intensities. Lattice determination and data collection were carried out using *XSCANS*, version 2.10b, software. All data reduction, including Lorentz and polarization corrections, and structure solution and graphics were performed using *SHELXTL PC*, version 4.2/360, software.[50] The structure refinement was performed using *SHELX 93* software.[50] All data were corrected for absorption using the ellipsoidal option in the *XEMP* facility of *SHELXTL PC*. A summary of the data collection parameters is given in Table 1.

The space group was determined to be the centric *C*2/*c*, using Patterson and difference Fourier techniques. This solution yielded all non-hydrogen atom positions. No hydrogen atoms were refined because of rotational motion of the hydroxide and ammonia groups about their metal bonds. The final refinement included anisotropic thermal parameters on all non-hydrogen atoms and converged to R1 = 0.0359 and wR2 = 0.0729.

dx.doi.org/10.1021/ic3020139 | *Inorg. Chem.* 2013, 52, 3547−3555

■ ASSOCIATED CONTENT

Supporting Information

X-ray crystallographic data for $[Co(NH_3)_6]_2[NpO_2(OH)_4]_3 \cdot H_2O$ in CIF format, ^{17}O NMR spectrum of $NpO_2(H_2O)_5^{2+}$ in an acid solution, and EXAFS curve fit data for $[Co(NH_3)_6]_2[NpO_2(OH)_4]_3 \cdot H_2O$. This material is available free of charge via the Internet at http://pubs.acs.org.

■ AUTHOR INFORMATION

Corresponding Author

*E-mail: dlclark@lanl.gov.

Notes

The authors declare no competing financial interest.

†R.J.D.: Deceased April 26, 2007.

■ ACKNOWLEDGMENTS

We thank Drs. H. J. Dewey, T. W. Newton, D. E. Morris, M. P. Neu, and W. Runde for helpful discussions. This work was supported by the Division of Chemical Sciences, Geosciences, and Biosciences, Office of Basic Energy Sciences, U.S. Department of Energy. Los Alamos National Laboratory is operated by Los Alamos National Security, LLC, for the National Nuclear Security Administration of the U.S. Department of Energy under Contract DE-AC52-06NA25396. All XAFS measurements were performed at the Stanford Synchrotron Radiation Lightsource (SSRL), a national user facility operated by Stanford University on behalf of the U.S. Department of Energy, Office of Basic Energy Sciences. Health Physics support at SSRL was provided by the Los Alamos National Laboratory section of the Seaborg Institute for Transactinium Studies.

■ REFERENCES

(1) *The Chemistry of the Actinide and Transactinide Elements*; Morss, L., Edelstein, N. M., Fuger, J., Eds.; Springer: Berlin, 2006.

(2) Grenthe, I.; Fuger, J.; Konings, R. J. M.; Lemire, R. J.; Muller, A. B.; Nguyen-Trung, C.; Warner, H. *Chemical thermodynamics of uranium*; Elsevier: Amsterdam, The Netherlands, 1992; Vol. *1*.

(3) Silva, R. J.; Bidoglio, G.; Rand, M. H.; Robouch, P. B.; Wanner, H.; Puigdomenech, I. *Chemical thermodynamics of americium*; Elsevier: Amsterdam, The Netherlands, 1995; Vol. *2*.

(4) Lemire, R. J.; Fuger, J.; Nitsche, H.; Potter, P.; Rand, M. H.; Rydberg, J.; Spahiu, K.; Sullivan, J. C.; Ullman, W. J.; Vitorge, P.; Warner, H. *Chemical thermodynamics of neptunium and plutonium*; Elsevier: Amsterdam, The Netherlands, 2001; Vol. *4*.

(5) Barney, G. S.; Delegard, C. H. *Proc. Am. Chem. Soc. Symp. Exp. Model. Stud.*; Actinide Speciation Non-Ideal Systems, 1999; p 83.

(6) Shilov, V. P. *Radiochemistry* **1998**, *40*, 11.

(7) Peretrukhin, V. F.; Shilov, V. P.; Pikaev, A. K. *Alkaline chemistry of transuranics elements and technetium and the treatment of alkaline radioactive wastes*; WCH-EP-0817, Westinghouse Hanford Company, 1995.

(8) Clark, D. L.; Conradson, S. D.; Donohoe, R. J.; Keogh, D. W.; Morris, D. E.; Palmer, P. D.; Rogers, R. D.; Tait, C. D. *Inorg. Chem.* **1999**, *38*, 1456.

(9) Wahlgren, U.; Moll, H.; Grenthe, I.; Schimmelpfennig, B.; Maron, L.; Vallet, V.; Gropen, O. *J. Phys. Chem. A* **1999**, *103*, 8257.

(10) Szabo, Z.; Grenthe, I. *Inorg. Chem.* **2007**, *46*, 9372.

(11) Vallet, V.; Wahlgren, U.; Schimmelpfennig, B.; Moll, H.; Szabo, Z.; Grenthe, I. *Inorg. Chem.* **2001**, *40*, 3516.

(12) Szabo, Z.; Grenthe, I. *Inorg. Chem.* **2010**, *49*, 4928.

(13) Buhl, M.; Schreckenbach, G. *Inorg. Chem.* **2010**, *49*, 3821.

(14) Schreckenbach, G.; Hay, P. J.; Martin, R. L. *Inorg. Chem.* **1998**, *37*, 4442.

(15) Shamov, G. A.; Schreckenbach, G. *J. Am. Chem. Soc.* **2008**, *130*, 13735.

(16) Hratchian, H. P.; Sonnenberg, J. L.; Hay, P. J.; Martin, R. L.; Bursten, B. E.; Schlegel, H. B. *J. Phys. Chem. A* **2005**, *109*, 8579.

(17) Tsushima, S. *Inorg. Chem.* **2012**, *51*, 1434.

(18) Antonio, M. R.; Williams, C. W.; Sullivan, J. A.; Skanthakumar, S.; Hu, Y.-J.; Soderholm, L. *Inorg. Chem.* **2012**, *51*, 5274.

(19) Bolvin, H.; Wahlgren, U.; Moll, H.; Reich, T.; Geipel, G.; Fanghaenel, T.; Grenthe, I. *J. Phys. Chem. A* **2001**, *105*, 11441.

(20) Williams, C. W.; Blaudeau, J. P.; Sullivan, J. C.; Antonio, M. R.; Bursten, B.; Soderholm, L. *J. Am. Chem. Soc.* **2001**, *123*, 4346.

(21) Grenthe, I.; Drozdzynski, J.; Fujino, T.; Buck, E. C.; Albrecht-Schmitt, T. E.; Wolf, S. F. In *The Chemistry of the Actinide and Transactinide Elements*, 3rd ed.; Morss, L., Edelstein, N. M., Fuger, J., Eds.; Springer: Berlin, 2006; Vol. 3, p 253.

(22) Moll, H.; Reich, T.; Szabo, Z. *Radiochim. Acta* **2000**, *88*, 411.

(23) Alcock, N. W.; Roberts, M. M.; Brown, D. *J. Chem. Soc., Dalton Trans.* **1982**, 33.

(24) Wilkerson, M. P.; Dewey, H. J.; Gordon, P. L.; Scott, B. L. *J. Chem. Crystallogr.* **2004**, *34*, 807.

(25) Alcock, N. W.; Roberts, M. M.; Brown, D. *J. Chem. Soc., Dalton Trans.* **1982**, 25.

(26) Grigor'ev, M. S.; Krot, N. N. *Radiochemistry* **2010**, *52*, 375.

(27) Vodovatov, V. A.; Lychev, A. A.; Mashirov, L. G.; Smolin, Y. I.; Shepelev, Y. F. *Radiokhimiya* **1987**, *29*, 146.

(28) Charushnikova, I. A.; Krot, N. N.; Starikova, Z. A. *Radiochemistry* **2007**, *49*, 565.

(29) Pauling, L. *The Nature of the Chemical Bond*, 3rd ed.; Cornell University Press: Ithaca, NY, 1960.

(30) Ankudinov, A. L.; Conradson, S. D.; Mustre de Leon, J.; Rehr, J. J. *Phys. Rev. B: Condens. Matter Mater. Phys.* **1998**, *57*, 7518.

(31) Ankudinov, A. L.; Rehr, J. J. *Phys. Rev. B: Condens. Matter Mater. Phys.* **1997**, *56*, R1712.

(32) Allen, P. G.; Shuh, D. K.; Bucher, J. J.; Edelstein, N. M.; Reich, T.; Denecke, M. A.; Nitsche, H. *Inorg. Chem.* **1996**, *35*, 784.

(33) Allen, P. G.; Bucher, J. J.; Clark, D. L.; Edelstein, N. M.; Ekberg, S. A.; Gohdes, J. W.; Hudson, E. A.; Kaltsoyannis, N.; Lukens, W. W.; et al. *Inorg. Chem.* **1995**, *34*, 4797.

(34) Catalano, J. G.; Brown, G. E., Jr. *Am. Mineral.* **2004**, *89*, 1004.

(35) Rehr, J. J.; Albers, R. C. *Rev. Mod. Phys.* **2000**, *72*, 621.

(36) Teo, B. K. *EXAFS: Basic Principles and Data Analysis*; Springer-Verlag: Berlin, 1986.

(37) Stern, E. A.; Sayers, D. E.; Lytle, F. W. *Phys. Rev. B: Solid State* **1975**, *11*, 4836.

(38) Madic, C.; Begun, G. M.; Hobart, D. E.; Hahn, R. L. *Inorg. Chem.* **1984**, *23*, 1914.

(39) Nakamoto, K. *Infrared and Raman Spectra of Inorganic and Coordination Compounds*; Wiley-Interscience: New York, 1997; Part A.

(40) Rabideau, S. W. *J. Phys. Chem.* **1963**, *67*, 2655.

(41) Nguyen-Trung, C.; Begun, G. M.; Palmer, D. A. *Inorg. Chem.* **1992**, *31*, 5280.

(42) Denning, R. G.; Norris, J. O. W.; Brown, D. *Mol. Phys.* **1982**, *46*, 287.

(43) Matsika, S.; Pitzer, R. M. *J. Phys. Chem. A* **2000**, *104*, 4064.

(44) Wilkerson, M. P.; Arrington, C. A.; Berg, J. M.; Scott, B. L. *J. Alloys Compd.* **2007**, *444–445*, 634.

(45) Wilkerson, M. P.; Berg, J. M. *Radiochim. Acta* **2009**, *97*, 223.

(46) Wilkerson, M. P.; Berg, J. M.; Hopkins, T. A.; Dewey, H. J. *J. Solid State Chem.* **2005**, *178*, 584.

(47) Appelman, E. H.; Kostka, A. G.; Sullivan, J. C. *Inorg. Chem.* **1988**, *27*, 2002.

(48) Zhurov, V. V.; Zhurova, E. A.; Stash, A. I.; Pinkerson, A. A. *J. Phys. Chem. A* **2011**, *115*, 13016.

(49) Wilkerson, M. P.; Burns, C. J.; Paine, R. T.; Scott, B. L. *Inorg. Chem.* **1999**, *38*, 4156.

(50) *XSCANS* and *SHELXTL PC* are products of Siemens Analytical X-ray Instruments, Madison, WI.